Available at www.sciencedirect.com

ScienceDirect

journal homepage: www.elsevier.com/locate/he

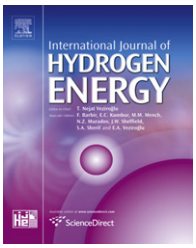

Design of a novel flat-plate photobioreactor system for green algal hydrogen production

*Bojan Tamburic, Fessehaye W. Zemichael, Paul Crudge, Geoffrey C. Maitland, Klaus Hellgardt**

Department of Chemical Engineering and Chemical Technology, Imperial College of Science, Technology and Medicine, London SW7 2AZ, UK

ARTICLE INFO

Article history:
Received 5 November 2010
Received in revised form
11 February 2011
Accepted 15 February 2011
Available online 1 April 2011

Keywords:
Flat-plate photobioreactor
Green algae
Hydrogen production
Renewable energy

ABSTRACT

Some green microalgae have the ability to harness sunlight to photosynthetically produce molecular hydrogen from water. This renewable, carbon-neutral process has the additional benefit of sequestering carbon dioxide and accumulating biomass during the algal growth phase. We document the details of a novel one-litre vertical flat-plate photobioreactor that has been designed to facilitate green algal hydrogen production at the laboratory scale. Coherent, non-heating illumination is provided by a panel of cool-white light-emitting diodes. The reactor body consists of two compartments constructed from transparent polymethyl methacrylate sheets. The primary compartment holds the algal culture, which is agitated by means of a recirculating gas-lift. The secondary compartment is used to control the temperature of the system and the wavelength of radiation. The reactor is fitted with probe sensors that monitor the pH, dissolved oxygen, temperature and optical thickness of the algal culture. A membrane-inlet mass spectrometry system has been developed and incorporated into the reactor for dissolved hydrogen measurement and collection. The reactor is hydrogen-tight, modular and fully autoclaveable.

1. Introduction

1.1. Green algal hydrogen production

There is urgent global demand for an energy carrier that is clean, renewable and available. Molecular hydrogen (H_2) is a fuel that has the potential to provide the clean energy required for transport, heating and electricity. The aim of the Solar Hydrogen Project at Imperial College London is to produce H_2 by a carbon-neutral, sustainable process that uses unlimited natural resources – sunlight and water [1]. The green alga *Chlamydomonas reinhardtii* (*C. reinhardtii*) has the ability to photosynthetically produce H_2 under anaerobic conditions [2]. Initially, photons are absorbed within the chloroplast of *C. reinhardtii*. This solar energy facilitates the photochemical oxidation of water into protons and molecular oxygen (O_2) by the photosystem II (PSII) photoactive cluster centre. Electrons generated in this process are transferred to the iron-hydrogenase enzyme, which catalyses proton-electron recombination to produce H_2. The process may be summarised by the equations below.

$$2H_2O \rightarrow O_2 + 4H + 4e^- \quad \textit{water oxidation} \tag{1}$$

$$4H^+ + 4e^- \rightarrow 2H_2 \quad \textit{proton} - \textit{electron recombination} \tag{2}$$

Iron-hydrogenase activity is inhibited in the presence of O_2, which implies that this direct biophotolysis process is self-limiting. In order to maintain continuous H_2 production, it is necessary to remove O_2 as it is being produced. Sulphur deprivation of *C. reinhardtii* diminishes its ability to repair PSII

* *Corresponding author*. Tel./fax: +44 0 2075945577.
E-mail addresses: bojan.tamburic@imperial.ac.uk (B. Tamburic), klaus.hellgardt@imperial.ac.uk (K. Hellgardt).
0360-3199/$ – see front matter
doi:10.1016/j.ijhydene.2011.02.091

Nomenclature

aq	aqueous solution
C. reinhardtii	unicellular green alga *Chlamydomonas reinhardtii*
DC	direct current
H_2	molecular hydrogen
LED	light-emitting diode
m/e	atomic mass-to-charge ratio
MIMS	membrane-inlet mass spectrometry
O_2	molecular oxygen
OD	optical density
PAR	photosynthetically active radiation
PBR	photobioreactor
Perspex	polymethyl methacrylate
PFA	perfluoroalkoxy (plastic pipe material)
pO_2	dissolved oxygen
PSII	photosystem II protein complex
PWM	pulse width modulation
TAP	tris-acetate-phosphate growth medium

proteins, thus reducing photosynthetic O_2 production below the level of respiratory O_2 consumption so that overall, O_2 is being used up [3]. The algal metabolism is therefore responsible for creating an anaerobic environment that leads to sustained H_2 production. This H_2 production can be sustained over a period of approximately five days because the algal cells deplete resources under anaerobic conditions.

Biohydrogen production is both renewable and sustainable. The microalgal feedstock is inexpensive and readily available, and the light intensity requirements for algal growth and H_2 production are modest, typically in the range of 40 W m^{-2} [4]. There is also the additional benefit of cultivating algal biomass lipids for subsequent biodiesel production, as well as the potential for temporary CO_2 sequestration within the algal cells. The main barriers to the commercialisation of green algal H_2 production are the low photochemical conversion efficiencies of the process and the prohibitive photobioreactor (PBR) costs [5].

1.2. *Photobioreactors*

Commercial growth of algal biomass (e.g. *Chlorella* and *Dunaliella*, grown for the pigmenting agent astaxanthin and β-carotene respectively) is normally restricted to inexpensive open systems such as natural ponds, circular ponds with a rotating arm for stirring, or raceway ponds [5,6]. During photobiological H_2 production it is necessary to efficiently harvest a highly mobile and diffusive gaseous molecule – an enclosed PBR is required. Enclosed PBRs also provide reproducible cultivation conditions, good heat transfer control, better biomass yield, better product quality and the opportunity for flexible technical design [7,8]. A typical PBR is essentially a four phase system consisting of the solid algal cells, the liquid growth medium, the gaseous H_2 product, and the superimposed light radiation field [9]. An understanding of the complex interaction between the biohydrogen production reaction and the associated environmental parameters such as the fluid dynamics and light transfer within the reactor is therefore required. The productivity of a closed PBR is limited by various design features, but most importantly the reactor needs to operate under favourable illumination conditions, with an optimised surface-to-volume ratio and light–dark cycle, and with adequate mass transfer properties [10]. The light intensity and wavelength incident on the PBR are both important, as are factors that determine the light dilution, light attenuation and light mixing throughout the system [11]. The PBR geometries regularly considered in the literature are the stirred-tank reactor [12,13], the vertical-column reactor [14,15], the horizontal tubular reactor [16,17] and the flat-plate reactor. A focused comparison of these PBR geometries is given in Table 1.

Flat-plate reactors are characterised by a high surface-to-volume ratio, which leads to the best photosynthetic efficiencies observed for any PBR [4]. Artificially illuminated flat-plate reactors are often vertical, with the light source incident on the reactor from one side. Outdoor flat-plate reactors are typically tilted at an angle that allows optimal exposure to solar irradiation [5]. The region immediately adjacent to the illuminated reactor surface is a photic zone where light saturation, and consequently the photoinhibition of algal growth and H_2 production processes, repeatedly occurs. In addition, the light energy available to algal cells decreases exponentially away from this photic zone – it has been estimated that for a fully grown culture of *C. reinhardtii*, effective light penetration is limited to a depth of 0.8 mm [15]. It is therefore important to minimise these light gradients and control the light-dark cycles of the algal cells by means of an effective agitation system [18]. Flat-plate reactors are subject to relatively low mass transfer rates because the space between panels, known as the light path, is restricted and this reduces the clearance efficiency of the dissolved O_2 produced by photosynthesis [19]. Good O_2 diffusion rates through the reactor are required to achieve optimal algal biomass growth. Flat-plate reactors provide operational flexibility as they may be run in both batch and continuous modes [6]. The height and width of flat-plate reactors are the two dimensions available for scale-up, but only up to a practical limit of 2–3 m [9]. Typical limitations of flat-plate reactors are the scaling-up requirements (the need for many compartments and support materials), the difficulty in controlling culture temperature, the possibility of algal cell clustering on the reactor wall, and the incompatibility with certain algal strains [19]. Algal cell clustering is prevalent near the top of vertical reactors with a fixed liquid level, such as vertical-column and flat-plate reactors featuring a gas-lift agitation system. Certain *C. reinhardtii* strains have a tendency to pellet to the bottom of the reactor and require energy-intensive mechanical agitation (such as shaking) to survive.

2. Reactor design

2.1. *Design specification*

The motivation for designing this PBR was to create a simple system that would enable quick measurement of the key

Table 1 – A comparison of the various photobioreactor geometries used to facilitate green algal H_2 production.

	Illumination	Mass transfer	H_2-tight	Scale-up	Economics
Pond	No process control; Natural illumination only	Low liquid cycling rate; Poor gas exchange	No	Limited only by available land area	Commercial Chlorella and Dunaliella growth
	×	××	×	✓✓✓	
Stirred-tank	Poor light diffusion; Artificial illumination only	High degree of liquid back-mixing; Mechanical agitation is energy-intensive	Yes	Internal illumination r equired	Scaled-up applications prohibitively expensive
	××	✓	✓	××	××
Vertical-column	Low surface-to-volume-ratio; Artificial illumination for efficient growth	Air-lift/bubble column provides good mixing; Low shear stress on algal cells	Yes	Illumination area decreases with size; Material selection difficult	Domestic microalgal and plankton growth; Many large-scale growth applications
	✓	✓✓✓	✓	×	✓✓
Tubular	Large illumination surface area; Conical/α geometries for outdoor operation	Large gas gradients arise along tubes	Yes	Additional sections added via manifolds; H_2-tight requirement limits material choice	Commercial Chlorella growth; Impractical for H_2 production applications
	✓✓	×	✓	✓	×
Flat-plate	Large surface-to-volume ratio; Inclined design for outdoor operation	Difficult to control light dilution gradients; Algal fouling possible	Yes	Operational flexibility; Two dimensions available for scale-up	Multiple units required; Some large-scale growth applications
	✓✓✓	✓✓	✓	✓✓	✓

parameters in the biohydrogen production process under carefully controlled conditions. As part of the design specification, the parameters that should be controlled and/or measured were selected. These parameters were used to drive the reactor design, and the process was completed by developing the ancillary systems and equipment required to service the reactor. The critical control parameters are light intensity, wavelength, temperature, agitation and mixing, and nutrient delivery and dilution [6]. Continuous, on-line measurement of H_2 production and H_2 collection is required. Additionally, it is necessary to measure the algal growth rate, the dissolved oxygen concentration (to determine if the culture is anaerobic), and the uptake rates of key nutrients such as sulphate and acetate (which largely governs the pH of the culture) [18].

Since the availability of light is normally the limiting factor for algal growth and H_2 production, we selected the reactor geometry that offers the highest surface-to-volume ratio – the vertical flat-plate reactor. Additional benefits of this geometry include the possibility of modular design, flexible operating conditions and potential future scale-up to a larger outdoor system. When selecting reactor materials, it was important to consider their strength, durability, spectral properties, toxicity to algal cells, and the permeability to H_2 [12]. The reactor was designed to be fully autoclaveable to minimise the possibility of contamination, and completely modular to allow easy cleaning and maintenance between experiments [20]. The choice of a minimalistic reactor design and the selection of materials and ancillary systems equipment were made with the intention of keeping the cost of this flat-plate reactor as low as possible, competitive with targets laid out in the literature [3].

The reactor ancillary systems were concerned with illumination, agitation, measurement, datalogging and the user control interface. Illumination was provided by a light-emitting diode (LED) array and the main challenge was to select the correct geometric configuration for optimal light exposure [15]. Diaphragm pumps were used to fulfil the agitation requirements by operating in the turbulent flow regime with appropriate mixing patterns and low levels of shear stress on the culture [5]. It was essential to provide instrumentation to measure the pH, dissolved oxygen (pO_2), H_2 production and algal growth rate [20]. In our system, commercial probes are used for *in situ* pH and pO_2 measurements: H_2 is measured by Membrane Inlet Mass Spectrometry (MIMS) and the algal growth rate is monitored by regularly measuring the optical thickness (or density) of the culture using a light meter or photodiode. Datalogging and user control interfaces are implemented by means of a National Instruments system.

2.2. *Dual-compartment design*

The novel dual-compartment flat-plate reactor, which was designed and constructed, is shown in Fig. 1. The reactor body was made of Perspex (polymethyl methacrylate), a transparent polymer alternative to glass that is relatively inexpensive, autoclaveable and easy to handle and process. The Perspex body consists of a 5 mm thick separator sheet sandwiched between a 25 mm thick front sheet and a 15 mm thick back sheet (Fig. 1a). Two rectangular compartments (primary and secondary) were machined into the front and back sheets respectively. The Solid Works design was programmed into

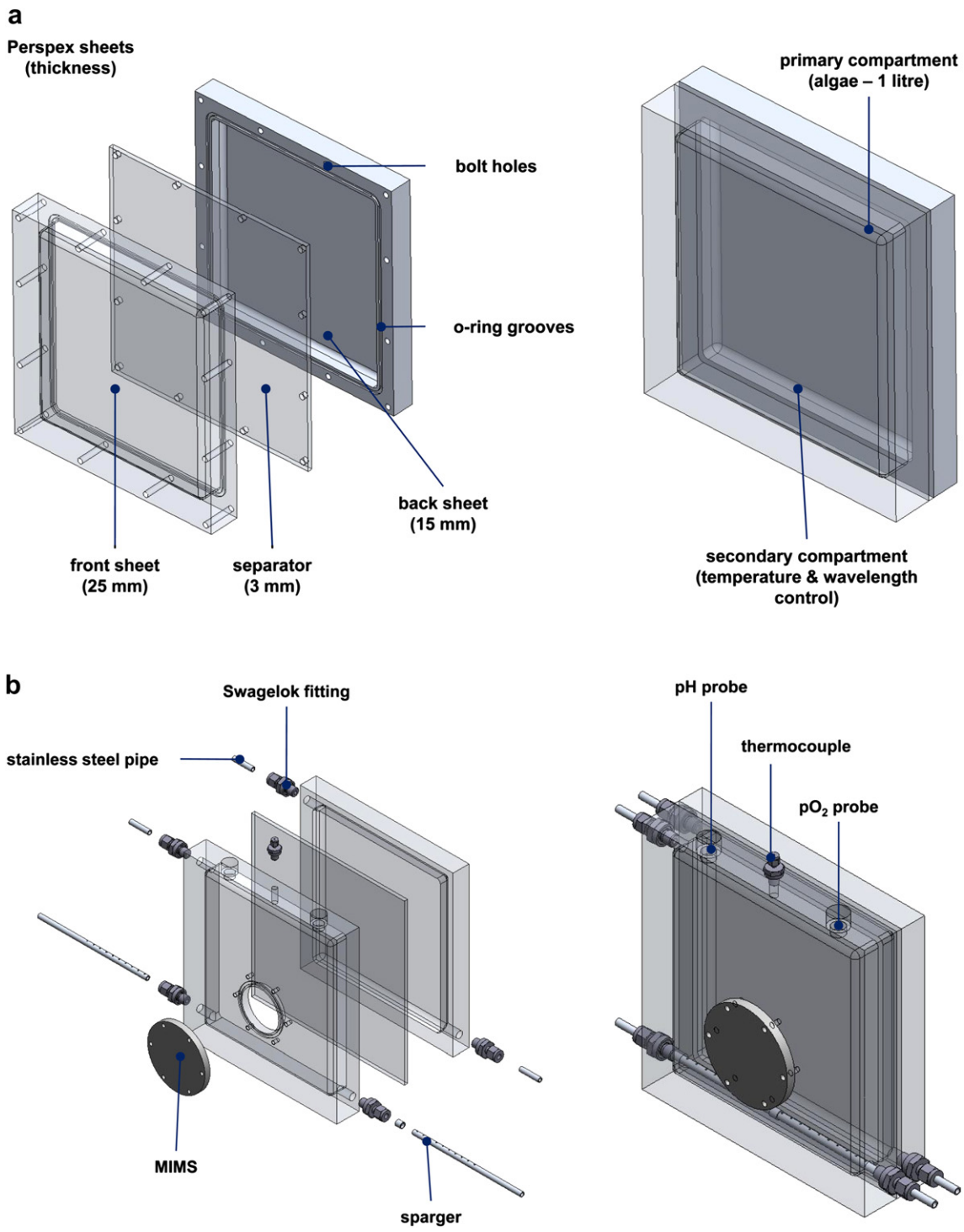

Fig. 1 – Novel dual-compartment vertical flat-plate reactor design (left: exploded view; right: assembled view). (a)Assembly of the primary and secondary reactor compartments from three machined Perspex sheets. (b)Addition of agitation system features and measuring instruments (c)Construction of the complete structure with reactor, base and LED array.

the computer-aided machining software Feature Cam, which was used to run the Hardinge VMC800II computer numerical control machine. This machine cut the required reactor features into the Perspex sheets. Perspex polish was applied to the machined surfaces to improve their optical transparency. A crucial element of the reactor design was that it should be impermeable to H_2. This means that special care had to be taken to ensure a good seal at all joints and points where devices and features were inserted through the reactor walls – at any location where the algal culture could potentially be exposed to the surroundings. The Perspex sheets were sealed with an inlaid grooved system of Viton fluoropolymer elastometer o-rings and compressed using a set of 12 stainless steel bolts. This layout also satisfied the

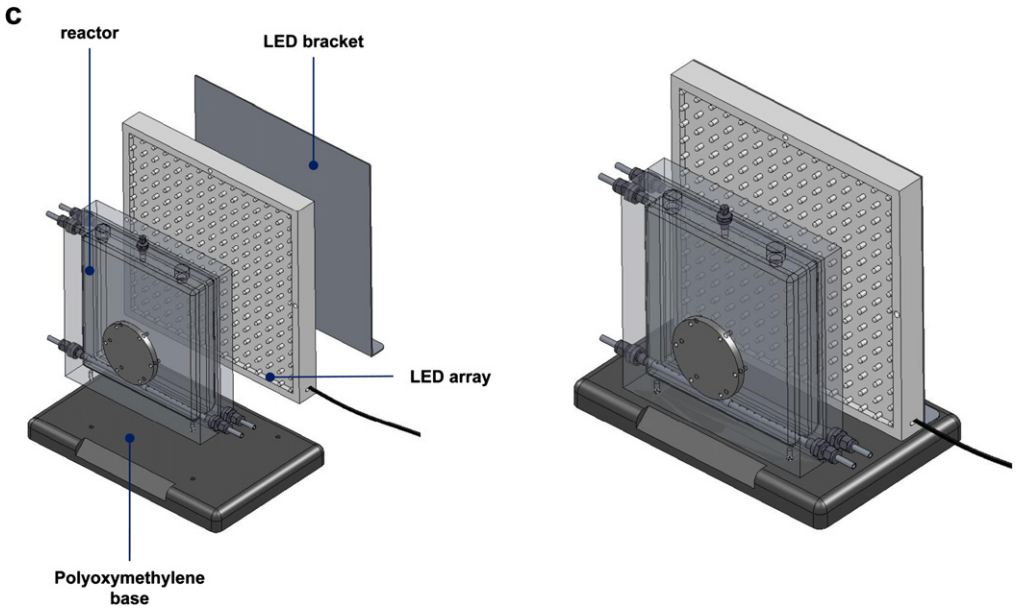

Fig. 1 – (*continued*).

requirements of a fully modular reactor design. The purpose of the primary compartment is to accommodate approximately one-litre of growing or hydrogen-producing algal culture. The secondary compartment is filled with water (or a light absorbing aqueous solution) and provides both the temperature and wavelength control for the system.

A recirculating gas-lift system provides the agitation to the *C. reinhardtii* culture in the primary compartment. The gas bubbling is introduced by means of a stainless steel sparger near the bottom of the compartment (Fig. 1b). A bi-directional flow of gas into the sparger provides an even pressure distribution within it, resulting in a well-balanced gas-lift profile. The gas leaves the compartment at the top of the reactor and is re-circulated. There is also liquid circulation in the secondary compartment; the liquid flows upwards from the bottom of the reactor. The holes in the reactor body required for the agitation system were sealed with stainless steel Swagelok fittings incorporating Viton o-rings. Viton fluoropolymer elastometer o-rings are known to seal very well against H_2 diffusion leaks, with a low deuterium permeability of 1.25×10^{-7} cm^3 s^{-1} cm^{-1} of material at standard temperature and pressure [21]. Swagelok fittings are leak-tight and made from stainless steel SS316, a material that is relatively common and non-corrosive. The measuring instruments (thermocouple, pO_2 and pH probes) are inserted via the appropriate slots at the top of the primary compartment. The MIMS system for H_2 measurement slots into the front of the reactor. These devices are all sealed by custom-made leak-tight o-ring connections. None of the materials in contact with the algal culture are known to be toxic to *C. reinhardtii* [15].

The entire structure is screw-connected onto a firm, black (matt, to minimise surface reflection) polyoxymethylene base, which also holds the LED array with the aid of a support bracket (Fig. 1c). The LED array selection is flexible – the main requirement is that it needs to be of the appropriate dimensions and intensity range/distribution (see section 3.1). There is also a constraint on the LED spread and brightness to ensure uniformity of illumination across the reactor. The final dual-compartment reactor body dimensions were $250 \times 240 \times 65$ mm (height × width × thickness), and the entire construction, including the base and LED array, could fit into a box with dimensions $270 \times 340 \times 220$ mm.

2.3. *Agitation system*

A standard liquid diaphragm pump from KNF Neuberger was used to circulate water, or a coloured aqueous solution, around the secondary compartment. The liquid diaphragm pump has a nominal flow rate of 0.3 l min^{-1}, but this rate is partially controllable by pulse width modulation (PWM) of the diaphragm frequency. The flow rate and inlet temperature of the secondary compartment are governed by the heat transfer properties of the reactor system, as discussed previously. The secondary compartment agitation system uses semi-transparent, flexible silicone tubing between the pump and the reactor body. The silicone tubing was slotted onto the reactor/pump inlet and outlet ports, and secured with zip cable ties to prevent it from slipping during operation.

Primary compartment agitation is provided by a turbulent gas-lift system emanating from a dual-entry stainless steel sparger at the bottom of the compartment (Fig. 2a). The gas flow system is enclosed in quarter-inch perfluoroalkoxy (PFA) plastic piping and circulated around the reactor so that no gaseous hydrogen is lost to the environment. PFA is a flexible polymer with an excellent seal against H_2 diffusion – its permeability to H_2 has been measured to be $(2.3 \pm 0.6) \times 10^{-6}$ cm^3 s^{-1} cm^{-1} [22]. Gas is circulated by means of a customised gas diaphragm pump from KNF Neuberger. This pump features a stainless steel pumping head with Swagelok inlet/outlet connections to minimise H_2 diffusion leaks in this critical region, as well as full PWM control of the pumping speed. The single gas diaphragm pump feeds both

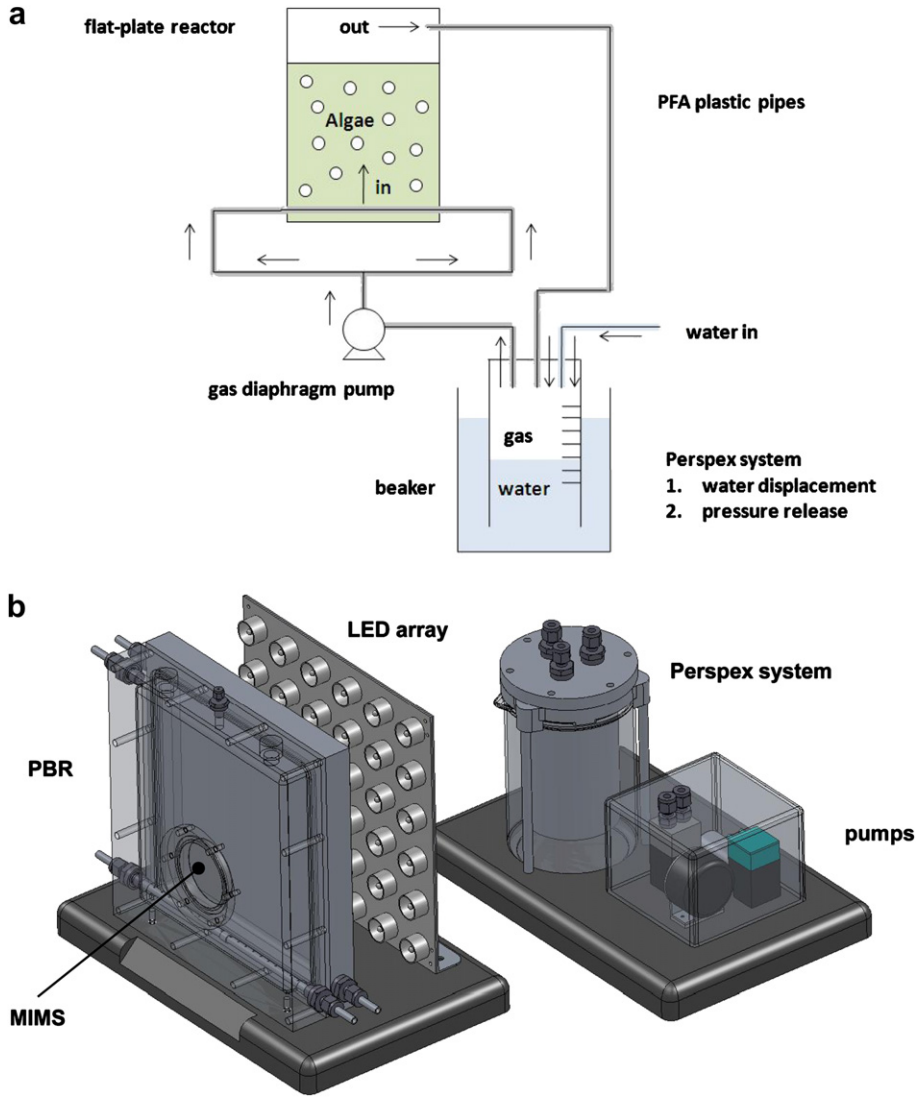

Fig. 2 – Agitation system in the flat-plate photobioreactor. (a) Gas-lift agitation in the primary compartment by means of a gas diaphragm pump, and incorporation of the Perspex water displacement and pressure release system. (b) Assembly of the main reactor body together with LED array and the ancillary agitation system components.

sparger inlets via a T-connector – in order to maintain a balanced flow distribution in the primary compartment, the two PFA pipes between the T-connector and each sparger inlet are of identical length. The sparger itself is constructed from a 240 mm long pipe of quarter-inch stainless steel, and it is perforated by 20 evenly-spaced circular holes, each with a diameter of 1 mm. Due to the physics of this layout, bubbles are more likely to emerge from the holes near the sides of the reactor. This produces a circular flow pattern towards the centre of the reactor, which provides good mixing to the algal culture. During the algal growth phase, the primary compartment may be agitated with a mixture of carbon dioxide and air, thus providing an additional carbon source for photomixotrophic algal growth. An inert gas such as argon may be used during the anaerobic H_2 production phase.

While being re-circulated between the gas diaphragm pump and the flat-plate PBR primary compartment, the agitation gas passes through a Perspex water displacement and pressure release system (Fig. 2a). This system consists of an inverted, graduated Perspex cylinder suspended over a glass beaker and partially filled with water. When the algae generate gas-phase products, either O_2 during photosynthetic growth or H_2 under anaerobic conditions, this additional volume is detectable as a downward displacement of water in the inverted cylinder. This arrangement also prevents the build-up of pressure in the PBR. Dissolved H_2 is also collected and analysed by a specially designed MIMS system, which is located on the front end of the primary compartment. The water displacement system, the liquid diaphragm pump and the gas diaphragm pump were mounted on their own polyoxymethylene base, behind the LED array (Fig. 2b). Stick-on rubber feet were applied to the base of the diaphragm pumps to act as vibration dampers.

2.4. *Membrane-inlet mass spectrometry*

Various methods have been used to monitor the gaseous species (O_2, CO_2 and H_2) involved during photobiological H_2 production. The conventional method has been to use *in situ*

Clark-type electrode measurements and/or analysis of gas samples by gas chromatography. MIMS is another analytical technique used to measure *in situ* concentrations of dissolved gases or volatile organic compounds in aqueous solutions [23]. The membrane system is the only interface between a liquid sample at atmospheric pressure and the vacuum chamber of a mass spectrometer. The membrane is made from different polymeric materials that allow gases to diffuse simultaneously or selectively depending on the investigation [24]. For selective H_2 diffusion, a semi-permeable polymer electrolyte membrane material such as Nafion is required. The technique allows direct comparison of the evolved gases and provides continuous monitoring of process conditions, i.e. light intensity, temperature, pH and system disturbances. Changes in these variables would be reflected in the MIMS gas concentration measurements. A MIMS system has been used in the literature to analyse relevant gases and determine the electron source during H_2 production by *C. reinhardtii* [25]. In that experiment, MIMS was used to accurately measure the concentration of H_2 produced by *C. reinhardtii* under standard anaerobic conditions as well as in the presence of the PSII inhibitor DCMU. Consequently, the authors were able to conclude that the majority of electrons required for H_2 production originate from the photosynthetic mechanism of *C. reinhardtii*.

Our flat-plate reactor utilises the Aston Analytical Ultra-Trace MIMS System. The mass spectrometer is a compact quadrupole Pfeiffer Vacuum Prisma, running Windows Quadstar 422 software. Gases dissolved in the liquid phase within the primary compartment of the flat-plate PBR diffuse through a thin polydimethylsiloxane membrane (permeable to all the gases involved) affixed on a disc holder inscribed with a perforated mesh (Fig. 3). The disk holder is sealed onto the stainless steel MIMS body by means of a Viton fluoropolymer elastometer o-ring. Inert gas (argon) introduced to the disc holder cavity directly carries diffused gaseous products, via a heatable capillary, into the mass spectrometer. To avoid any damage to the vacuum system, a moisture trap is fitted before the inlet to the mass spectrometer. Apart from the direct measurement of gaseous products kinetics, the MIMS system offers the additional benefits of potential H_2 separation and collection, as well as the reduction of possible H_2 induced inhibition of the biophotolytic H_2 production process [25].

MIMS extracts H_2 from the algal culture by a three-stage process called pervaporation. In the first step, H_2 molecules produced in the reactor are absorbed onto the membrane surface; this is followed by the permeation of these H_2 molecules through the membrane material, and finally by their desorption into the argon carrier gas stream on the other side [26]. A modified form of Fick's First Law [27] (Eq. (3)) has been used to calculate the H_2 pervaporation rate through the membrane. This H_2 pervaporation rate of 9.3 ml h^{-1} is significantly higher than the 2.0 ml h^{-1} (per litre of culture) wild-type *C. reinhardtii* H_2 production rate typically quoted in the literature [3,4,18]. Consequently, any H_2 produced by the algae is rapidly stripped out of the system by MIMS – the rate of H_2 extraction through the membrane is equivalent to the H_2 production rate inside the reactor. MIMS has therefore been calibrated entirely in the gas-phase by substituting the H_2 pervaporating through the membrane/reactor interface with a known flow rate of hydrogen gas from a cylinder. A Porter VCD 1000 mass flow meter was used to control the flow rate of hydrogen gas, and a linear correlation between this flow rate and the mass spectrometer signal was determined. Calibrated MIMS H_2 production results are shown in Section 3.4.

$$k_{trans} = (P \cdot A \cdot \Delta p)/l \quad (3)$$

where, P (H_2 permeability) $= 6 \times 10^{-15}$ m^2 s^{-1} Pa^{-1}
A (membrane surface area) $= 1.36 \times 10^{-3}$ m^2
l (membrane thickness) $= 3.20 \times 10^{-4}$ m
Δp (H_2 partial pressure) $= 1$ atm
k_{trans} (H_2 pervaporation rate) $= 9.3$ ml h^{-1}

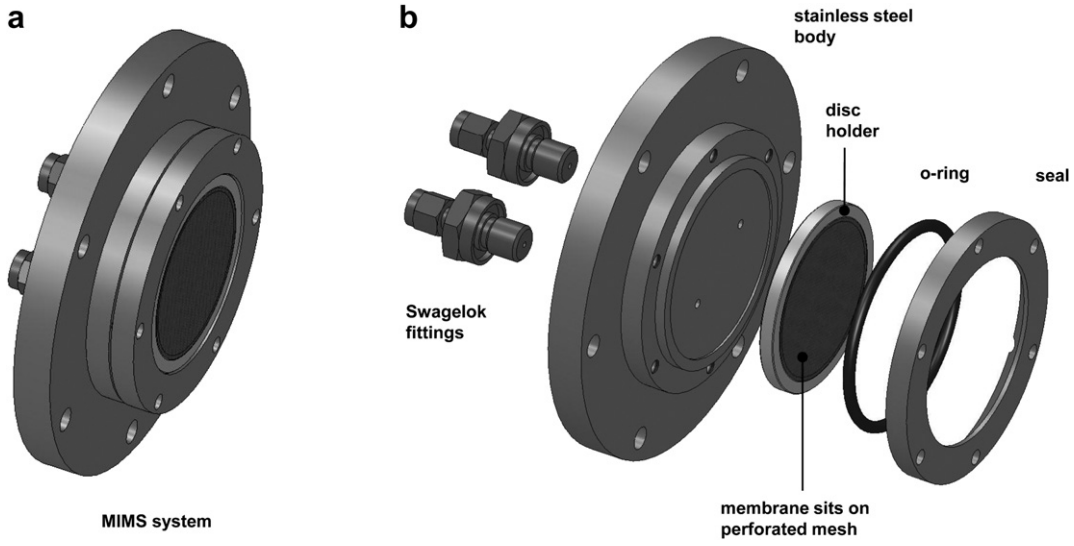

Fig. 3 – Design of the Membrane Inlet Mass Spectrometry (MIMS) system. (a) The complete MIMS system, which slots into the front of the flat-plate PBR primary compartment, extracts dissolved gases and sends them to a mass spectrometer for analysis. (b) MIMS exploded view – the membrane sits on a perforated disc mesh, which is fixed to the stainless steel body by means of an o-ring seal.

2.5. Datalogging and control

The key parameters that affect the H_2 production by *C. reinhardtii* include the pH, pO_2, temperature and OD of the culture. pH and pO_2 are measured using commercial probes from Consort – the SZ10T galvanic pO_2 electrode and the SP10T pH electrode. The temperature in the algal compartment is measured with a K-type thermocouple from Omega. The optical thickness is monitored using a photodiode with an absorption bandwidth of 650–700 nm. The photodiode detects the LED light-scattering by the algae in the photosynthetically active region of the light spectrum. All of these measurement devices can be recorded using the National Instruments datalogging system; this system has also been set up to control the ancillary PBR equipment such as the LED array, the liquid diaphragm pump and the gas diaphragm pump (Fig. 4). The datalogging and control system is centred on the National Instruments Compact RIO. This device contains a real-time controller unit as well as its own independent hard drive, which may be programmed via an Ethernet connection to a computer running Lab View software. The Compact RIO controller is powered by a 24 V direct current (DC) power supply, and it is connected to an eight-slot chassis, which carries various system-specific input/output modules.

The pH and pO_2 electrodes, as well as the photodiode signal, are datalogged with the NI-9205 analogue input module. It is necessary to use the PHTX pre-amplifier from Omega to increase the impedance of the electrode signals to 20 kΩ and make them compatible with the analogue input module specifications. All three of these raw voltage signals required calibration. The pH signal was measured in two buffer solutions of known pH values (pH 4.01 and pH 9.12) and assigned those values – the remainder of the pH scale was then interpolated linearly. The pO_2 signal was set to 0% in nitrogen-saturated water and 100% in oxygen-saturated water – the pO_2 consequently takes a percentage value based on the oxygen saturation of the liquid. The photodiode signal was calibrated against the output of a light meter placed at the same location. The thermocouple is datalogged with the NI-9211 thermocouple analogue module. In this case, the module intrinsically carries out the calibration according to NIST-certified standards and a temperature output is obtained. The PBR system uses a 24 V DC Brightest Day Light White LED array from LED Wholesalers and a 12 V DC NF30 KPDC liquid diaphragm pump from KNF Neuberger. Both of these devices may be controlled by PWM at a frequency of 1 kHz using an NI-9474 high-speed sourcing digital output module. However, due to the mismatch in input voltages, two separate NI-9474 modules are required. The PM24766 – NMP830 gas diaphragm pump from KNF Neuberger has been specifically designed for PWM control with a 0.9–5.0 V signal, which is provided by the NI-9401 TTL digital input/output module. In summary, the National Instruments Compact RIO runs the datalogging and control system in real-time with the aid of five input/output modules: NI-9205, NI-9211, NI-9474 (24 V), NI-9474 (12 V) and NI-9401 (Fig. 4).

3. Results and discussion

3.1. Light intensity distribution

Overall, *C. reinhardtii* cells have modest light intensity requirements – the growth, sulphur deprivation and H_2 production processes need no more than 200 μE s^{-1} m^{-2} of photosynthetically active radiation (PAR) – about 40 W m^{-2} [2]. Algal cells that remain in the dark for extended periods (dark zone) or that become overexposed to illumination (photic zone) will not grow or produce H_2 efficiently. The photic zone corresponds to an illumination exceeding 100 W m^{-2}, although this value is algal strain dependent [3]. The objective is therefore to supply all *C. reinhardtii* cells with uniform illumination of the appropriate

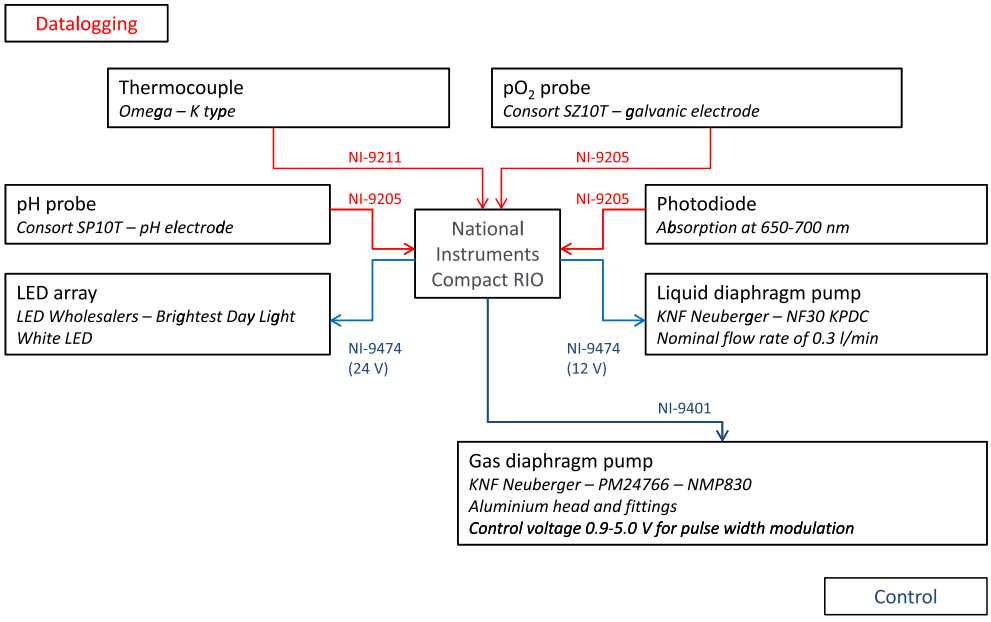

Fig. 4 – Datalogging and control system architecture using the National Instruments Compact RIO real-time embedded controller and modular chassis.

intensity [28]. An LED array provides illumination that is uniform, coherent, efficient and non-heating, all desirable properties for the flat-plate PBR. An LED array panel, approximately 200 × 200 mm in size, was purchased from LED Wholesalers. Its light intensity is varied using the National Instruments datalogging and control system. A light meter, operating on integrating sphere principles, was used to measure the spatial light intensity distribution of the LED array (operating at maximum power) (Fig. 5). The spatial light intensity distribution, measured across a plane parallel to – and located at a distance of 30 cm directly away from – the cool-white LED array, appeared relatively constant across the surface area of measurement, with a light intensity of 58 ± 3 W m^{-2} (Fig. 5, top surface). When the Perspex flat-plate PBR was placed between the LED array and the light meter, the light intensity fell to 43 ± 8 W m^{-2} (Fig. 5, bottom surface). This result is primarily due to limitations in the transparency of machined Perspex, but there is also evidence of additional shading effects radially away from the reactor centre. It is therefore important to provide sufficient agitation to cycle the algal culture through all parts of the reactor in order to prevent the build-up of localised light gradients, and to ensure that the majority of algal cells receive the illumination they require. It is also possible to use a light meter or photodiode in a similar setup as described above to measure the optical density (OD) of the culture, which is directly proportional to the algal growth rate [28]. The optical density, or absorbance, of a liquid is a quantity used to describe the transmission of light through that liquid. The Beer–Lambert law describes the optical density as a logarithmic ratio between the light intensity incident on the liquid (I_{in}) and the light intensity transmitted through the liquid (I_{out}):

$$OD = -\log_{10}(I_{out}/I_{in}) \quad Beer - Lambert\ Law \tag{4}$$

3.2. Wavelength modulation

A spectrophotometer was used to analyse *C. reinhardtii* absorption in the visible region of the electromagnetic spectrum and a light meter was used to measure the corresponding cool-white LED emission spectrum. The spectral match between the *C. reinhardtii* absorption and LED emission is shown in Fig. 6a; the absorption and emission spectra have been normalised by setting the area under both curves equal to unity. There are two major light absorption mechanisms in *C. reinhardtii* – the carotenoid absorption in the 400–500 nm spectral range and the PSII absorption in the red region of the spectrum centred on the 663 nm peak; the algae also reflect green light. PSII absorption is a threshold mechanism, that is to say the algae could use photons of any wavelength ≤680 nm for photosynthesis, but preferentially use 663 nm, as evidenced by the strong absorption peak at this wavelength [4]. The cool-white LED array provides powerful, well-balanced illumination over the entire visible spectrum, but a closer look at the normalised LED emission spectrum reveals a significant spectral mismatch with *C. reinhardtii* absorption in the green and red regions of the spectrum. This could potentially cause unnecessary over-saturation at non-PAR wavelengths, resulting in photo-inhibition of the algal growth and H_2 production processes [15].

It is therefore important to incorporate the capacity to modulate wavelength into green algal PBR design. This could be accomplished by changing the LED array itself, but a more practical solution is to apply a light filter between the cool-white LED array and the main reactor body. The dual-compartment flat-plate reactor design offers the possibility to modulate wavelength without any external filters, while at the same time providing temperature control for the reactor system. Aqueous solutions (*aq*) of various coloured ions may

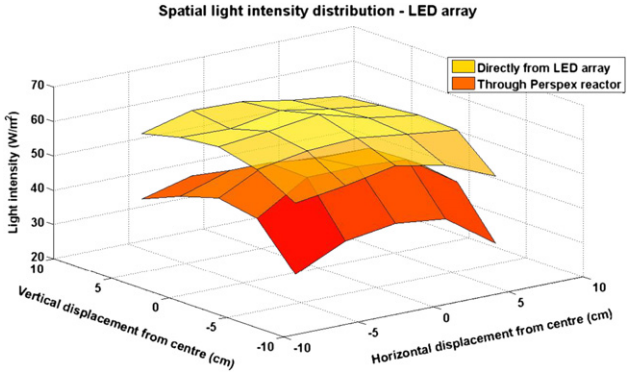

Fig. 5 – Variations in the spatial light intensity distribution across a plane parallel to – and located at a distance of 30 cm away from – the cool-white LED array.
• Directly from the LED array (top surface)
• Through the Perspex flat-plate photobioreactor (bottom surface).

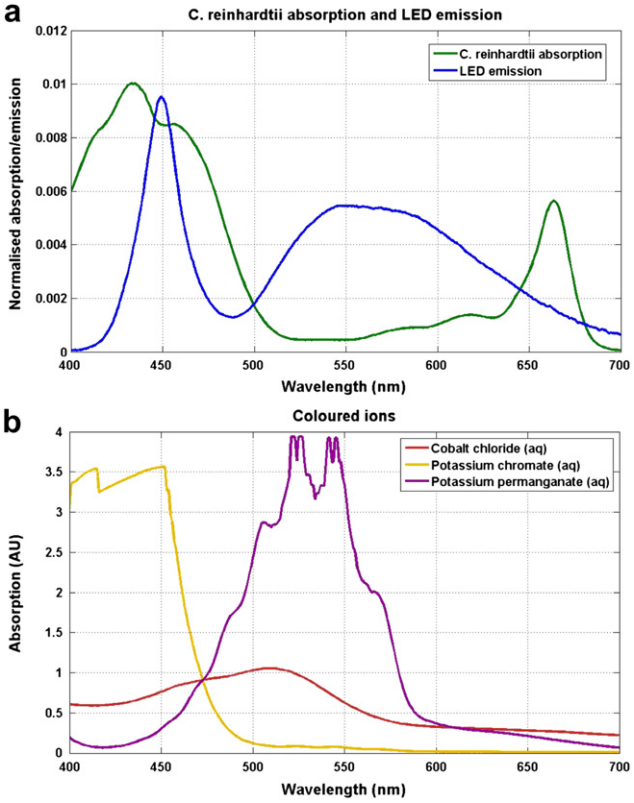

Fig. 6 – Use of the secondary compartment for LED wavelength modulation. (a) Spectral match between the (normalised) LED emission and *C. reinhardtii* absorption. (b) Absorption spectra of some common coloured aqueous solutions that can be used to modulate LED wavelength.

be circulated around the secondary compartment to modulate the wavelength of LED illumination incident on the algal culture in the primary compartment (Fig. 6b). For example, the purple potassium permanganate (*aq*) may be used to reduce any photoinhibition of PSII by filtering out the suboptimal green light. Orange potassium chromate (*aq*) could be used to switch-off parts of the carotenoid absorption spectrum in order to investigate the involvement of carotenoids in the growth of *C. reinhardtii* and the ability of xanthophylls cycle pigments to protect *C. reinhardtii* cells [29]. Concentrated red cobalt chloride (*aq*) could be used to combine the above effects.

3.3. *Heat transfer*

The secondary compartment of the flat-plate PBR may be used to control the temperature of the algal culture. A simple model was developed in Comsol multiphysics modelling and simulation software to examine the heat transfer properties of the PBR, focussing on estimating the Perspex wall thickness, inlet temperature and flow rate that could be used to maintain the appropriate primary compartment temperature for *C. reinhardtii* cultivation (Fig. 7). This model features a number of simplifications – it is based on a two-dimensional vertical cross-section through the reactor body, and agitation is assumed to take place in the secondary compartment only, with the inlet and outlet located in this same two-dimensional plane. Within this model, the secondary compartment is represented by the rectangular cavity on the left of Fig. 7 and the primary compartment by the larger rectangular cavity on the right; they are separated and insulated by a layer of Perspex. Mass transfer in the secondary compartment follows the incompressible Navier–Stokes equation, with no pressure and no viscous stress present at any point in the compartment, and gravity acting downwards on the water jet rising from the inlet at the bottom. The model predicts laminar flow throughout the secondary compartment, and the water jet slows down and spreads out on the way up. The physics of mass transfer was coupled to convective and conductive heat transfer in the secondary compartment by means of the inlet velocity, so that the water jet transfers heat upwards through the compartment. The heat transfer properties are strongly influenced by the physical properties of water and Perspex listed below.

	Water	Perspex
Density, ρ	1000 kg m^{-3}	1190 kg m^{-3}
Viscosity, η	8.9 10^{-4} Pa s	–
Conductivity, k	0.58 W m^{-1} K^{-1}	0.2 W m^{-1} K^{-1}
Heat capacity, C_p	2108 J kg^{-1} K^{-1}	1450 J kg^{-1} k^{-1}

The conductive heat transfer coefficient of Perspex, h, is also of primary importance and it varies linearly with Perspex thickness – it takes a value of 5.8 W m^{-2} K^{-1} in the case of a 3 mm thick sheet and a value of 3.4 W m^{-2} K^{-1} for a 10 mm thick sheet [30]. The heat transfer is principally governed by the heat flux boundary condition between surfaces at different temperatures. For example, in the Perspex boundary layer between the secondary compartment and the surroundings, heat flows into the Perspex layer based on the temperature of the water in the secondary compartment and it flows out of the layer based on the temperature of the surroundings, thus determining the temperature distribution within the Perspex layer itself. This information may be summarised by the heat flux (Eqns. 5–7).

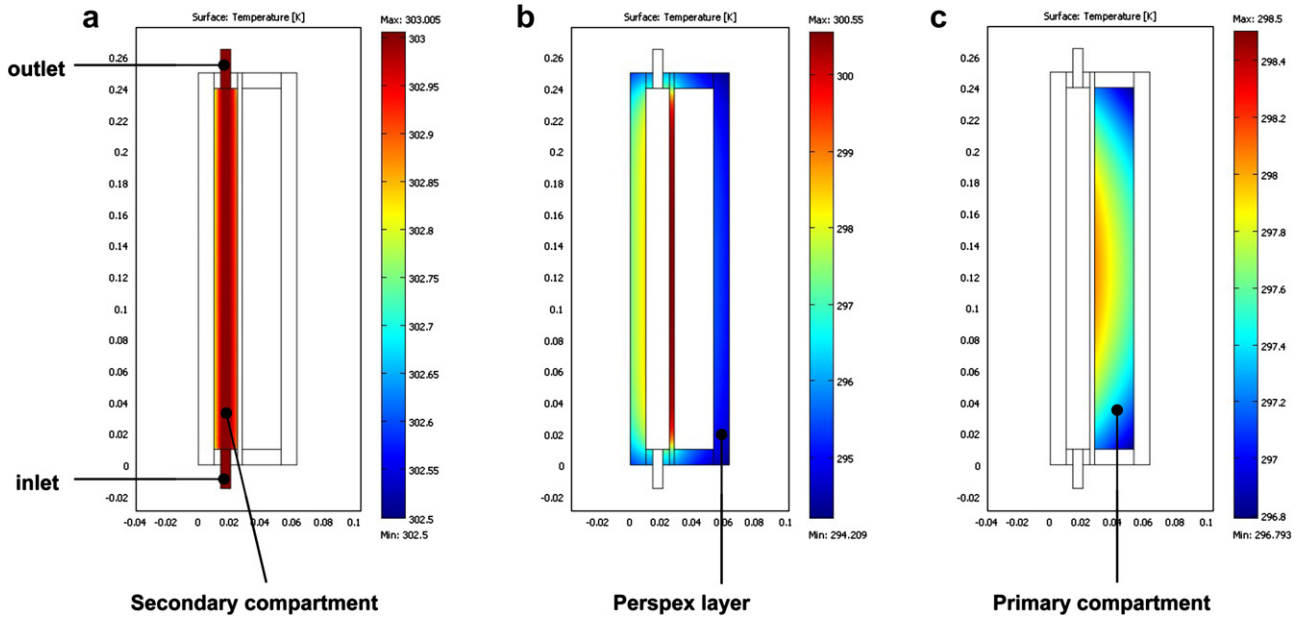

Fig. 7 – Two-dimensional (vertical cross-section) model of the heat transfer through the flat-plate photobioreactor. (a) Mass flow driven convection and conduction in the secondary compartment. (b) Conduction through the Perspex layers. (c) Convection and conduction in the primary (algal) compartment.

Table 2 – A comparison between the primary compartment temperature as predicted by the Comsol model, and measured experimentally for different pump flow rates and secondary compartment temperatures.

Pump flow rate (l min^{-1}) controlled	$T_{secondary}$ (°C) controlled	$T_{primary}$ (°C) predicted by model	$T_{primary}$ (°C) measured	$\Delta T_{primary}$ (°C) calculated
0.30	10	15.6	15.4	- 0.2
0.30	20	21.2	20.9	- 0.3
0.30	30	27.3	27.9	+ 0.6
0.30	40	33.4	34.7	+ 1.3
0.15	10	15.3	15.0	- 0.3
0.15	20	21.1	20.4	- 0.7
0.15	30	27.5	28.7	+ 0.8
0.15	40	33.8	35.0	+ 1.2

$$\textit{Heat flux, } q = h \cdot \Delta T \tag{5}$$

$$q = h \cdot (T_{water} - T_{perspex}) \quad \textit{inner boundary of Perspex layer} \tag{6}$$

$$q = h \cdot (T_{surroundings} - T_{perspex}) \quad \textit{outer boundary of Perspex layer} \tag{7}$$

Fig. 4 shows the results of this Comsol heat transfer model for a specific set of input parameters. With a vertical inflow velocity of 0.155 m s^{-1} (calculated from the nominal pump flow rate of 0.3 l min^{-1}) and an inlet temperature of 303 K (30 °C), the secondary compartment appears well-insulated, cooling only by a fraction close to the Perspex boundaries and creating a temperature differential of approximately 0.2 K in the compartment (Fig. 7a). Conductive heat transfer takes place in the Perspex layer between the two compartments and the surroundings. Assuming an ambient temperature of 293 K (20 °C), good heat transfer within the 5 mm Perspex separator between the two compartments was observed. The temperature differential in the Perspex layer was approximately 6 K, and the greatest heat loss to the surroundings occurred through the back of the reactor, i.e. away from the primary compartment (Fig. 7b). Assuming conductive and convective heat transfer, as well as ideal mixing in the primary compartment, the mean temperature of the algae may be calculated to be 297.6 K (24.6 °C) (Fig. 7c). The model allows variables such as inflow velocity, inlet temperature and Perspex layer thickness to be modified and computes the corresponding change in the temperature of the algal culture. An experiment was conducted to provide a comparison between the primary compartment temperature predicted by the model and the corresponding temperature measured experimentally (Table 2). The ambient temperature during this experiment was 23 °C. The pump flow rate was controlled by the NI system and the secondary compartment temperature was controlled and measured using a Grant LTC1 heating/cooling water bath unit. The temperature in the water bath therefore takes a constant pre-set value and all heat transfer takes place subsequently as the water is pumped around via the secondary compartment. The primary compartment temperature was measured using a K-type thermocouple.

The results show that primary compartment temperatures of 15–35 °C are easily attained and controlled – this is the accepted temperature range for *C. reinhardtii* growth [4]. The model is correct to ±1.3 °C in all instances, usually significantly better. The experimental data also reveals that a longer residence time distribution in the secondary compartment (resulting from a lower flow rate) gives slightly better temperature control, an effect that is also seen by the model. The model is therefore useful in providing a holistic overview of the heat transfer properties in the flat-plate reactor. In reality, the reactor is actually better at controlling primary compartment temperature than the model predicts. The model would need to be extended to a more complex three-dimensional geometry with gas-lift agitation introduced in the primary compartment before the numerical values resulting from the model may be considered completely reliable.

3.4. *Hydrogen production*

An illustrative result obtained with this reactor system is shown in Fig. 8. It demonstrates that the novel flat-plate reactor is suitable for *C. reinhardtii* hydrogen production, and that it is capable of monitoring the key parameters of this process. The wild-type laboratory strain CC-124 *C. reinhardtii* was used in the illustrative experiment. Sulphur deprivation was achieved by centrifugation. In this process, algal cells were pelleted at the bottom of the centrifugation vessel by centrifugation at 3000 rotations per minute for 20 min [31]. The sulphur-rich tris-acetate-phosphate (TAP) algal growth medium was drained off and the algal cells were re-suspended in the sulphur-free TAP-S medium. Constant cool-white LED irradiation of 8.6 W m^{-2} (20% of the maximum irradiation available, see Fig. 5) was applied during the course of this experiment. Additionally, the temperature of the primary compartment was controlled at 20.0 °C. The dissolved oxygen concentration was measured using a calibrated galvanic pO_2 electrode. MIMS was used to measure the partial pressures of a number of dissolved gasses in the culture. This was achieved by using the mass spectrometer to observe the ion current generated at specific atomic masses corresponding to the gaseous compounds of interest, which include argon, water vapour, nitrogen, oxygen, carbon dioxide and hydrogen. The anaerobic H_2 production rate was observed by measuring the ion current at an atomic mass-to-charge ratio (m/z) of 2 units and calibrating the system as described in Section 2.4.

In the first 22 h of *C. reinhardtii* sulphur deprivation, the dissolved oxygen in the system was used up (Fig. 8b). The reason for this was that the rate of O_2 consumption by respiration had exceeded the rate of O_2 production by photosynthesis, so that overall, O_2 was being used up. As expected, hydrogen production began only once anaerobic conditions were established in the reactor. The sigmoid (logistic) shape of the hydrogen accumulation curve was similar to that described by Melis et al. [3]. The final volume of H_2 produced, measured to be 105 ml per litre of culture, is consistent with other wild-type *C. reinhardtii* H_2 production yields recorded in the literature [31,32]. The H_2 production rate, which is proportional to the MIMS ion current signal, was also measured continuously and *in situ* (Fig. 8a). The maximum H_2

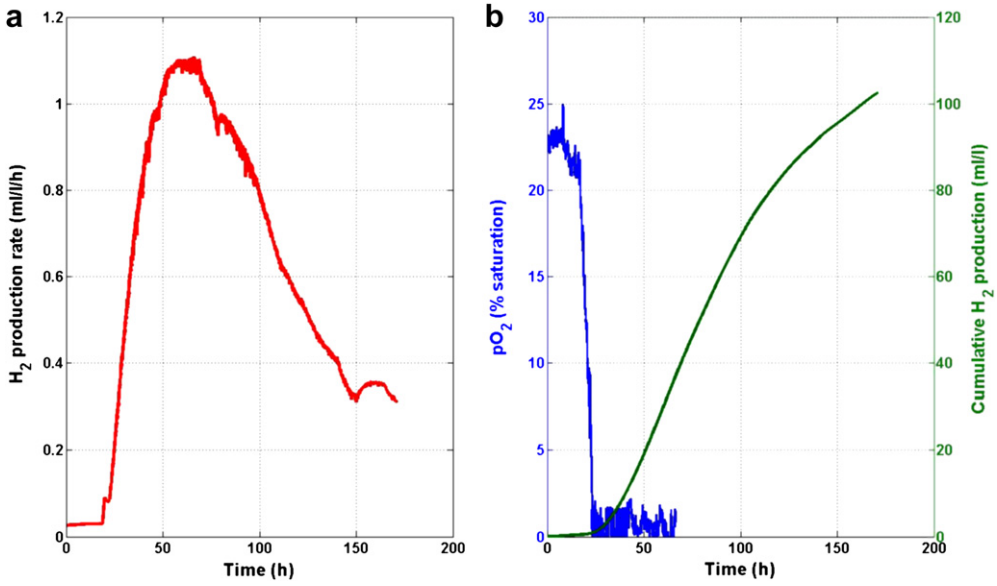

Fig. 8 – Results of an illustrative experiment carried out in the flat-plate photobioreactor: (a) CC-124 *C. reinhardtii* H_2 production rate measured by Membrane Inlet Mass Spectrometry (MIMS). (b) Cumulative H_2 production by CC-124 *C. reinhardtii* under anaerobic conditions.

production rate of 1.1 ml/l/h was observed approximately 60 h into the experiment. Since wild-type *C. reinhardtii* rates of up to 2.0 ml/l/h have been measured [3], there is space to improve the H_2 production rate in this reactor by optimising process conditions such as initial algal cell density, light intensity, wavelength, temperature and pH.

$$\text{Photochemical conversion efficiency} = \left(H_2 \text{ production rate } \left[l \cdot s^{-1}\right] \times H_2 \text{ energy content } \left[J \cdot l^{-1}\right] \times\right) \Big/ \text{Absorbed energy } \left[J \cdot s^{-1}\right] \quad (8)$$

It is also possible to use these experimental results together with the reactor irradiation data to calculate the photochemical conversion efficiency of the algae (Eq. (8)) [33]. Photochemical conversion efficiency determines the percentage of the energy carried by PAR incident on the algal culture that is converted into chemical energy stored in the released hydrogen molecules [4]. Given that the active reactor surface area is 0.048 m^2, and using the maximum H_2 production rate of 1.1 ml/l/h, together with the higher heating value for H_2 (141.86 J l^{-1}), a photochemical conversion efficiency of 0.24% has been calculated. This value is better than the 0.13% photochemical conversion efficiency obtained by Fouchard et al. [34], but it falls short of the 1.08% efficiency achieved by Giannelli et al. [33]. The latter obtained a similar H_2 yield at a lower light intensity by growing the algal culture to a higher cell density. Optimising these and other parameters will be the focus of future work with the flat-plate photobioreactor.

4. Conclusion

A flat-plate vertical one-litre photobioreactor that facilitates the biophotolytic H_2 production process has been designed and constructed. A comprehensive literature review has identified the advantages and limitations of various reactor geometries. The flat-plate reactor geometry was subsequently chosen due to its superior surface-to-volume ratio, which results in the highest observed photochemical efficiencies for H_2 production. The reactor enables rapid and accurate measurements of the key parameters in the biohydrogen production process, such as cell density, pO_2 and pH, under carefully controlled conditions. A novel dual-compartment flat-plate reactor was constructed from Perspex, using hydrogen-impermeable o-rings and stainless steel fittings. The primary compartment holds the algal culture and contains the key measuring instruments, including the MIMS system developed for *in situ* H_2 detection and extraction. The secondary compartment is used to control the system temperature and wavelength. Turbulent culture mixing is achieved by a circulating gas-lift system that is operated with a customised liquid diaphragm pump, while a cool-white LED array provides uniform, coherent, non-heating illumination to the system. A comprehensive real-time datalogging and control system has been developed. An illustrative H_2 production experiment achieved a H_2 yield of 105 ml/l at a maximum H_2 production rate of 1.1 ml/l/h and a photochemical conversion efficiency of 0.24%. From July to November 2010, the reactor was operated and demonstrated in the Antenna Exhibition of contemporary science at the London Science Museum.

Acknowledgements

The Solar Hydrogen project is funded by the UK Engineering and Physical Sciences Research Council (EPSRC).

Appendix

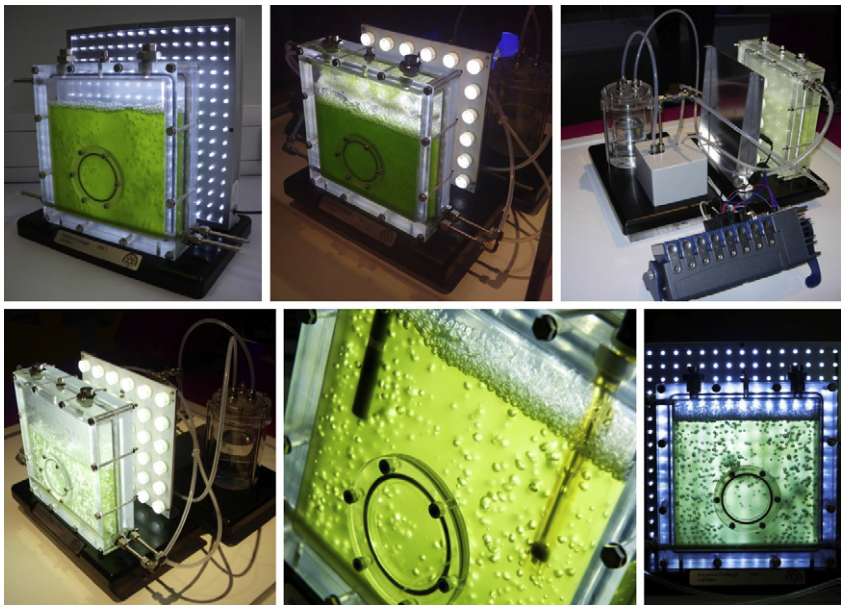

Fig. 9 – Photographs of the complete and operational dual-compartment flat-plate photobioreactor.

REFERENCES

[1] Tamburic B, Zemichael FW, Maitland GC, Hellgardt K. Parameters affecting the growth and hydrogen production of the green alga Chlamydomonas reinhardtii. Int J Hydrogen Energ; 2010;. doi:10.1016/j.ijhydene.2010.11.074.

[2] Ghirardi ML, Zhang L, Lee JW, Flynn T, Seibert M, Greenbaum E, et al. Microalgae: a green source of renewable H_2. Trends Biotechnol 2000;18:506–11.

[3] Melis A. Green algal hydrogen production: progress, challenges and prospects. Int J Hydrogen Energ 2002;27:1217–28.

[4] Akkerman I, Janssen M, Rocha J, Wijffels RH. Photobiological hydrogen production: photochemical efficiency and bioreactor design. Int J Hydrogen Energ 2002;27:1195–208.

[5] Carvalho AP, Meireles LA, Malcata FX. Microalgal reactors: a review of enclosed system design and performances. Biotechnol Progr 2006;22:1490–506.

[6] Pulz O. Photobioreactors: production systems for phototrophic microorganisms. Appl Microbiol Biot 2001;57:287–93.

[7] Ugwu CU, Aoyagi H, Uchiyama H. Photobioreactors for mass cultivation of algae. Bioresour Technol 2008;99:4021–8.

[8] Borowitzka MA. Commercial production of microalgae: ponds, tanks, tubes and fermenters. J Biotechnol 1999;70: 313–21.

[9] Posten C. Design principles of photo-bioreactors for cultivation of microalgae. Eng Life Sci 2009;9:165–77.

[10] Tsygankov AA. Laboratory scale photobioreactors. Appl Biochem Micro 2001;37:333–41.

[11] Uyar B, Eroglu I, Yucel M, Gunduz U, Turker L. Effect of light intensity, wavelength and illumination protocol on hydrogen production in photobioreactors. Int J Hydrogen Energ 2007; 32:4670–7.

[12] Skjanes K, Knutsen G, Kallqvist T, Lindblad P. H_2 production from marine and freshwater species of green algae during sulphur deprivation and considerations for bioreactor design. Int J Hydrogen Energ 2008;33:511–21.

[13] Berberoglu H, Yin J, Pilon L. Light transfer in bubble sparged photobioreactors for H_2 production and CO_2 mitigation. Int J Hydrogen Energ 2007;32:2273–85.

[14] Xu Z, Dapeng L, Yiping Z, Xiaoyan Z, Zhaoling C, Wei C, et al. Comparison of photobioreactors for cultivation of Undaria pinnatifida gametophytes. Biotechnol Lett 2002;24: 1499–503.

[15] Janssen M, Tramper J, Mur LR, Wijffels RH. Enclosed outdoor photobioreactors: light regime, photosynthetic efficiency, scale-up and future prospects. Biotechnol Bioeng 2003;81: 193–210.

[16] Molina EM, Fernandez FG, Camacho FG, Rubio FC, Chisti Y. Scale-up of tubular photobioreactors. J Appl Phycol 2000;12: 355–68.

[17] Dasgupta CN, Gilbert JJ, Lindblad P, Heidorn T, Borvang SA, Skjanes K, et al. Recent trend on the development of photobiological processes and photobioreactors for the improvment of hydrogen production. Int J Hydrogen Energ 2010;35:10218–38.

[18] Hankamer B, Lehr F, Rupprecht J, Mussgnug JH, Posten C, Kruse O. Photosynthetic biomass and H_2 production by green algae: from bioengineering to bioreactor scale-up. Physiol Plantarum 2007;131:10–21.

[19] Sierra E, Acien FG, Fernandez JM, Garcia JL, Gonzales C, Molina E. Characterization of a flat plate photobioreactor for the production of microalgae. Chem Eng J 2008;138:136–47.

[20] Nedbal L, Trtilek M, Cerveny J, Komarek O, Pakrasi HB. A photobioreactor system for precision cultivation of photoautotrophic microorganisms and high-content analysis of suspension dynamics. Biotechnol Bioeng 2008; 100:902–10.

[21] Derrick RG, McIntyre RL. Permeability of Teflon polytetrafluroethylene resin and buna-N butadiene-nitrile rubber to deuterium. J Chem Eng Data 1974;19:48–51.

[22] Extrand CW, Monson L. Gas permeation resistance of a perfluoroalkoxy-tetrafluoroethylene copolymer. J Appl Polym Sci 2006;100:2122–5.
[23] Scott RI, Williams TN, Whitmore TN, Lloyd D. Direct measurement of methanogenesis in anaerobic digesters by membrane-inlet mass spectrometry. Appl Microbiol Biotechnol 1983;18:236–41.
[24] Cournac L, Mus F, Bernard L, Guedeney G, Vignais P, Peltier G. Limiting steps of hydrogen production in *Chlamydomonas reinhardtii* and *Synechocystis* PCC 6803 as analysed by light-induced gas exchange transients. Int J Hydrogen Energ 2002; 27:1229–37.
[25] Hemschemeier A, Melis A, Happe T. Analytical approaches to photobiological hydrogen production in green algae. Photosynth Res 2009;102:523–40.
[26] Lloyd D, Thomas KL, Cowie G, Tammam JD, Williams AG. Direct interface of chemistry to microbiological systems: membrane inlet mass spectrometry. J Microbiol Methods 2002;48:289–302.
[27] Beckmann K, Messinger J, Badger MR, Wydrzynski T, Hillier W. On-line mass spectrometry: membrane inlet sampling. Photosynth Res 2009;102:511–22.
[28] Perner-Nochta I, Posten C. Simulations of light intensity variations in photobioreactors. J Biotechnol 2007;131:276–85.
[29] Bohne F, Linden H. Regulation of carotenoid biosynthesis genes in response to light in *Chlamydomonas reinhardtii*. Biochim Biophys Acta 2002;1579:26–34.
[30] Ashby MF. Materials selection in mechanical designs. 3rd ed. Elsevier; 2005. 519.
[31] Ghirardi ML, Dubini A, Yu J, Maness PC. Photobiological hydrogen-producing systems. Chem Soc Rev 2009;38:52–61.
[32] Kotay SM, Das D. Biohydrogen as a renewable energy source – Prospects and potentials. Int J Hydrogen Energ 2008;33: 258–63.
[33] Giannelli L, Scoma A, Torzillo G. Interplay between light intensity, chlorophill concentration and culture mixing on the hydrogen production in sulfur-deprived *Chlamydomonas reinhardtii* cultures grown in laboratory photobioreactors. Biotechnol Bioeng 2009;104:76–90.
[34] Fouchard S, Pruvost J, Degrenne B, Legrand J. Investigation of H_2 production using the green microalga *Chlamydomonas reinhardtii* in a fully controlled photobioreactor fitted with on-line gas analysis. Int J Hydrogen Energ 2008;33:3302–10.